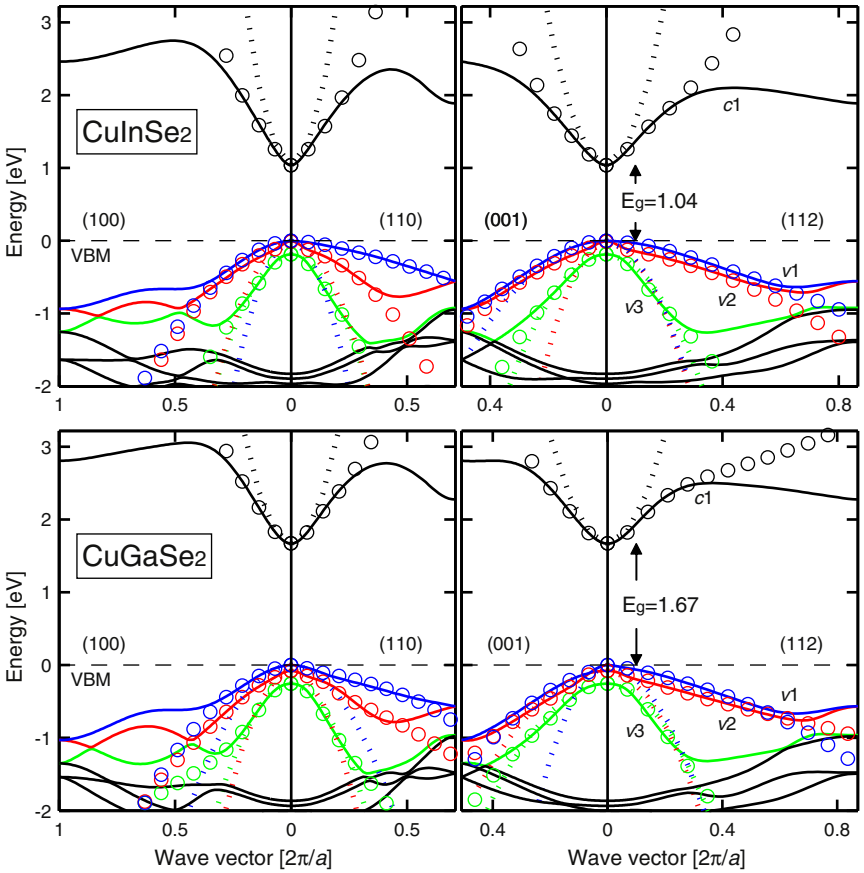

Fig. 1. Electronic band structure $E_j(\mathbf{k})$ of $CuInSe_2$ (upper panels) and $CuGaSe_2$ (lower panels) along the four symmetry directions (100), (110), (001), and (112). The energies referred to the VBM (dashed lines). The notation of the energy bands ($j = c1$, $v1$, $v2$, and $v3$) at the band edges refers to a spin-independent band indexing, where $c1$ represents the lowest CB and $v1$ represents the topmost VB. These VBs are highlighted with colors in the online version. The solid lines show the full-potential results from Refs. [1] and [2], the dotted lines represent the parabolic approximation of Eq. (1), and the circles are the fitted results of Eq. (2). Notice that the two uppermost VBs are badly described by the parabolic approximation in the main (100), (110), and (112) symmetry directions. Here, the notation of the symmetry directions (k_x, k_y, and k_z) is in units of $2\pi/a$, $2\pi/a$, and $2\pi/c$.

where e is the elementary charge and positive (negative) sign is for the CB (VBs). We have verified in this study that the ellipsoidal energy dispersion (Table 1) is valid for all four considered energy bands ($j = c1$, $v1$, $v2$, and $v3$) in the very vicinity of the Γ-point. However, away from the Γ-point, the parabolic approximation (dotted lines in Figs. 1 and 2) obviously fails to describe the energy dispersion of the VBs, especially for the topmost band in the (110) and (112) directions.

A common way to parameterize the energy bands is within the so called $\mathbf{k}\cdot\mathbf{p}$ approximation [7]. For cubic materials with twofold degenerate cation-*s*–anion-*p* bonding-like VBM the (spin-independent) energy dispersion has the form [7,8] $E_j(\mathbf{k}) = E_j^{pb}(\mathbf{k}) \pm \Delta \cdot (\delta \cdot (k_x^2 k_y^2 + k_y^2 k_z^2 + k_z^2 k_x^2) + k^4)^{1/2}$, and the corresponding expression for hexagonal structure is of the form $E_j(\mathbf{k}) = E_j^{pb}(\mathbf{k}) \pm \Delta \cdot (\delta \cdot k_\perp^4 + 1)^{1/2}$. However, the disadvantage with this method is that even for rather simple materials (like cubic or hexagonal SiC [8]) the parameterized bands can describe the VBs only close to the Γ-point. $CuIn_{1-x}Ga_xSe_2$ has a VBM involving Cu-*d*–Se-*p* antibonding-like state, and the crystal-field interaction as well as the spin-orbit coupling generates rather complex (anisotropic and non-parabolic) energy dispersions (Figs. 1 and 2). Therefore, the regular $\mathbf{k}\cdot\mathbf{p}$ approximation is not a sufficient method for describing the energy bands of $CuIn_{1-x}Ga_xSe_2$ down to ~0.5 eV below VBM. Instead, we start extend the $\mathbf{k}\cdot\mathbf{p}$ expressions to higher orders and with lower band symmetries, choosing the form $E_j(\mathbf{k}) = E_j^{pb}(\mathbf{k}) + \sum_{\alpha,n} \Delta_{\alpha,n} \cdot (\delta_{\alpha,n} \cdot k_\alpha^{2n} + 1)^{1/n}$. Each term alone describes a parabolic dispersion, but the higher order terms affect the dispersion for the larger wave vectors away from the Γ-point. Thus, the combination of terms can therefore describe how local effects (like crystal field and spin-orbit coupling) re-shape the energy dispersion, that otherwise would be parabolic. We find that the following expression is suitable to describe the energy bands of $CuIn_{1-x}Ga_xSe_2$ down to ~0.5 eV below VBM:

$$
\begin{aligned}
E_j(\mathbf{k}) = E_j^{pb}(\mathbf{k}) + E_j^0 + \Delta_{j,1}\left(\delta_{j,1}^2\left(\frac{\tilde{k}_x^4 + \tilde{k}_y^4}{m_0^2}\right) + \delta_{j,2}^2\left(\frac{\tilde{k}_x^2 \tilde{k}_y^2}{m_0^2}\right) + 1\right)^{1/2} \\
+ \Delta_{j,2}\left(\delta_{j,3}^3\left(\frac{\tilde{k}_x^6 + \tilde{k}_y^6}{m_0^3}\right) + \delta_{j,4}^3\left(\frac{\tilde{k}_x^2 \tilde{k}_y^4 + \tilde{k}_x^4 \tilde{k}_y^2}{m_0^3}\right) + 1\right)^{1/3} \\
+ \Delta_{j,3}\left(\delta_{j,5}^2\left(\frac{\tilde{k}_z^4}{m_0^2}\right) + 1\right)^{1/2} + \Delta_{j,4}\left(\delta_{j,6}^3\left(\frac{\tilde{k}_z^6}{m_0^3}\right) + 1\right)^{1/3} \\
+ \Delta_{j,5}\left(\delta_{j,7}^2\left(\frac{\tilde{k}_x^2 \tilde{k}_z^2 + \tilde{k}_y^2 \tilde{k}_z^2}{m_0^2}\right) + 1\right)^{1/2} \\
+ \Delta_{j,6}\left(\delta_{j,8}^3\left(\frac{\tilde{k}_x^4 \tilde{k}_z^2 + \tilde{k}_y^4 \tilde{k}_z^2}{m_0^3}\right) + \delta_{j,9}^3\left(\frac{\tilde{k}_x^2 \tilde{k}_z^4 + \tilde{k}_y^2 \tilde{k}_z^4}{m_0^3}\right) + \delta_{j,10}^3\left(\frac{\tilde{k}_x^2 \tilde{k}_y^2 \tilde{k}_z^2}{m_0^3}\right) + 1\right)^{1/3}.
\end{aligned}
\tag{2}
$$

Unfortunately, the rather complex VB energy dispersions of $CuIn_{1-x}Ga_xSe_2$ require quite many fitting parameters (Eq. (2) and Table 2). The CB, however, needs less parameters.

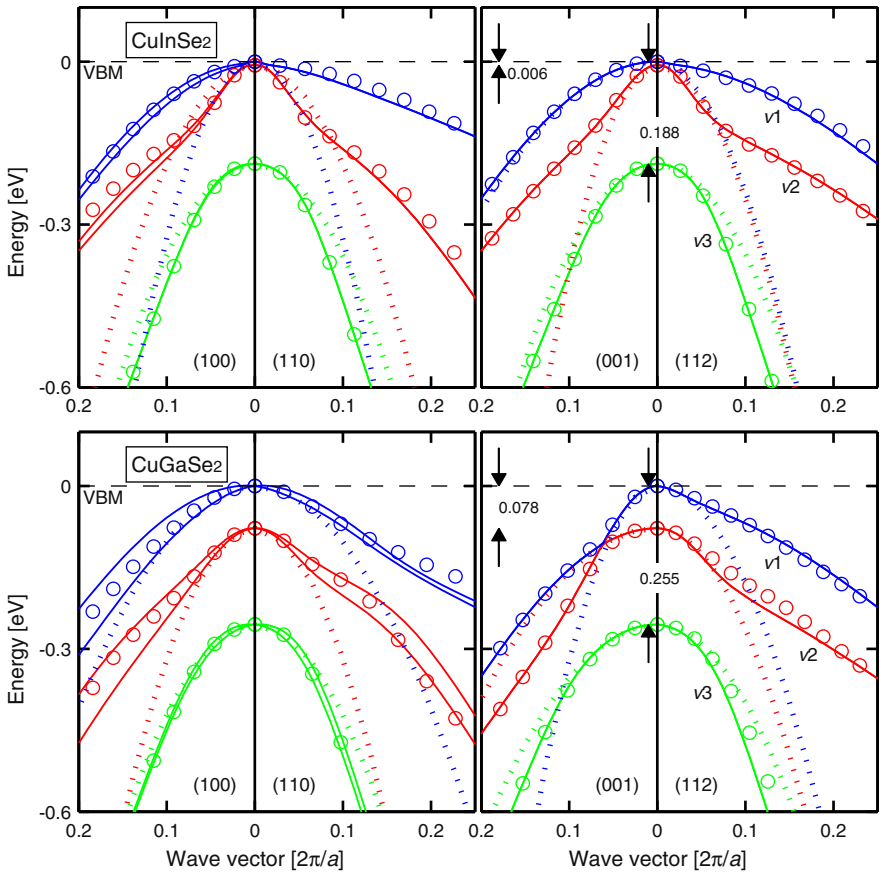

Fig. 2. Close-up of Fig. 1 demonstrating the strong non-parabolicity of the topmost VBs. Our parameterized energy bands $E_j(\mathbf{k})$ consider the average of the two spinor states $\psi_j^{\sigma}(\mathbf{k})$ with $\sigma = \downarrow$ and $\uparrow$, although there is a relatively large split of the spin-up- and spin-down-like bands in the (100)-direction; this average approximation is justified by $\psi_j^{\downarrow}(-\mathbf{k}) = \psi_j^{\uparrow}(\mathbf{k})$. Thus, the notation of the energy bands is $j = c1$, $v1$, $v2$, and $v3$ (where $c1$ represents the lowest CB and $v1$ represents the topmost VB) refers to a spin-independent band indexing.

Table 1
Parameters of Eq. (1) to describe the parabolic energy dispersions of the lowest CB and the three uppermost VBs in the vicinity of the Γ-point. $E_{v1}(\mathbf{0})$ is the VBM and $E_{c1}(\mathbf{0})$ is the fundamental band-gap energy E_g.

$CuIn_{1-x}Ga_xSe_2$	$x = 0.0$				$x = 0.5$				$x = 1.0$			
	$c1$	$v1$	$v2$	$v3$	$c1$	$v1$	$v2$	$v3$	$c1$	$v1$	$v2$	$v3$
$E_j(\mathbf{0})$ [eV]	0.97	0.00	0.01	0.19	1.20	0.00	0.02	0.20	1.47	0.00	0.08	0.26
$m_j^{\perp}$ [m_0]	0.08	0.14	0.25	0.27	0.10	0.40	0.17	0.29	0.13	0.47	0.20	0.29
$m_j^{\parallel}$ [m_0]	0.09	0.66	0.12	0.28	0.11	0.14	0.61	0.40	0.13	0.15	0.61	0.49

Table 2
Parameters of Eq. (2) to describe the non-parabolic contribution to the energy dispersions $E_j(\mathbf{k})$ of the lowest CB and the three uppermost VBs. The notation of the energy bands ($j = c1$, $v1$, $v2$, and $v3$) refers to a spin-independent band indexing, where $c1$ represents the bottommost CB and $v1$ represents the topmost VB (see Figs. 1 and 2).

$CuIn_{1-x}Ga_xSe_2$	$x = 0.0$				$x = 0.5$				$x = 1.0$			
	$c1$	$v1$	$v2$	$v3$	$c1$	$v1$	$v2$	$v3$	$c1$	$v1$	$v2$	$v3$
E_j^0 [eV]	−4.010	−5.311	−5.242	−5.620	−4.146	−6.210	−6.426	−5.835	−3.927	5.284	−5.789	−2.783
$\Delta_{j,1}$ [eV]	−0.295	0.006	−0.002	−0.021	−0.230	0.106	1.321	−0.026	−0.454	0.116	1.284	1.194
$\Delta_{j,2}$ [eV]	0	0.098	0.104	0.308	0	0.002	0.096	0.386	0	−10.771	−0.837	−0.024
$\Delta_{j,3}$ [eV]	−0.242	0.018	0.124	−0.025	−0.293	0.937	−0.017	−0.838	−0.419	0.088	0.347	−0.303
$\Delta_{j,4}$ [eV]	0	0.188	0.076	0.238	0	0.021	0.163	0.789	0	0.076	−0.051	0.608
$\Delta_{j,5}$ [eV]	−0.016	−0.048	0.001	−0.009	−0.046	0.001	0.011	0.370	−0.047	0.022	0.274	0.374
$\Delta_{j,6}$ [eV]	0	0.037	−0.073	0.117	0	−0.022	−0.313	−0.012	0	−0.111	−0.525	−4.362
$\delta_{j,1}$ [eV^{-1}]	30.669	952.000	2304.147	94.139	27.157	5.517	1.029	57.007	11.865	10.526	9.269	3.839
$\delta_{j,2}$ [eV^{-1}]	47.374	1754.386	4587.156	220.556	44.506	13.610	0.413	153.435	20.262	28.545	21.582	6.232
$\delta_{j,3}$ [eV^{-1}]	0	3.970	72.296	11.746	0	487.805	46.950	8.489	0	0.131	9.116	59.625
$\delta_{j,4}$ [eV^{-1}]	0	3.688	123.274	18.078	0	1128.668	72.844	13.509	0	0.126	21.328	148.516
$\delta_{j,5}$ [eV^{-1}]	31.852	6.041	56.004	64.137	21.124	1.314	247.158	7.921	12.978	7.709	12.141	8.014
$\delta_{j,6}$ [eV^{-1}]	0	3.134	6.100	12.031	0	267.523	29.076	8.743	0	64.185	66.808	5.309
$\delta_{j,7}$ [eV^{-1}]	222.641	37.004	3846.154	206.148	79.879	3322.259	212.902	16.836	76.319	236.742	16.240	5.092
$\delta_{j,8}$ [eV^{-1}]	0	12.647	16.269	6.982	0	92.954	4.885	57.890	0	31.947	6.710	1.209
$\delta_{j,9}$ [eV^{-1}]	0	61.565	33.169	34.114	0	118.064	0.000	273.400	0	34.784	4.831	1.394
$\delta_{j,10}$ [eV^{-1}]	0	46.679	31.275	32.237	0	110.327	6.074	153.523	0	40.765	5.243	2.124

The parameterized energy bands (circles in Figs. 1 and 2) can fairly accurately describe the energy bands for energies ~0.5 eV below the VBM and ~0.5 eV above the CB minimum (CBM). The energy difference of the two uppermost VBs at the Γ-point is only $E_{v1}(\mathbf{0}) - E_{v2}(\mathbf{0}) = 6$, 18, and 78 meV for $CuInSe_2$, $CuIn_{0.5}Ga_{0.5}Se_2$, and $CuGaSe_2$, respectively. These two VBs interact in this energy region which affects the band curvatures, and thus making the bands non-parabolic and anisotropic. Therefore, the parabolic approximation (represented by the Γ-point effective hole masses) is strictly valid only for energies to about −4, −10, and −40 meV below the VBM for $CuInSe_2$,$CuIn_{0.5}Ga_{0.5}Se_2$, and $CuGaSe_2$, respectively (see Fig. 2).

The CB has a rather spherical energy dispersion close to the Γ-point (i. e., $m_{c1,\perp} \approx m_{c1,\parallel}$; [1]). Since the CB is a single band, it is expected that the band is more parabolic and isotropic compared with the VBs. This is true, but already at an energy about 0.05 eV above the CBM $E_{c1}(\mathbf{0})$, the band becomes both non-parabolic and anisotropic (e. g. Fig. 1). This is a consequence of the crystal potential that makes the CB flat at about 50% out from the Γ-point in the first BZ. Our fitting using Eq. (2) can describe this non-parabolicity and the anisotropicity to describe the CB to about ~50% of the first BZ. However, the fitting cannot describe the flat curvature in the remaining part of the BZ in especially the (100) direction.

3. Effective electron and hole masses

From the parameterized energy bands of Eq. (2), the effective electron and hole mass tensors $m_j(\mathbf{k}) = \pm\hbar^2/(\partial^2 E_j(\mathbf{k})/\partial\mathbf{k}^2)|_{\mathbf{k}}$ were determined along the four symmetry directions. In Fig. 3, we present the inverse of the mass $m_j(\mathbf{k})^{-1}$for better visibility; for instance, the mass goes to infinity (whereas inverse mass is zero) when the energy

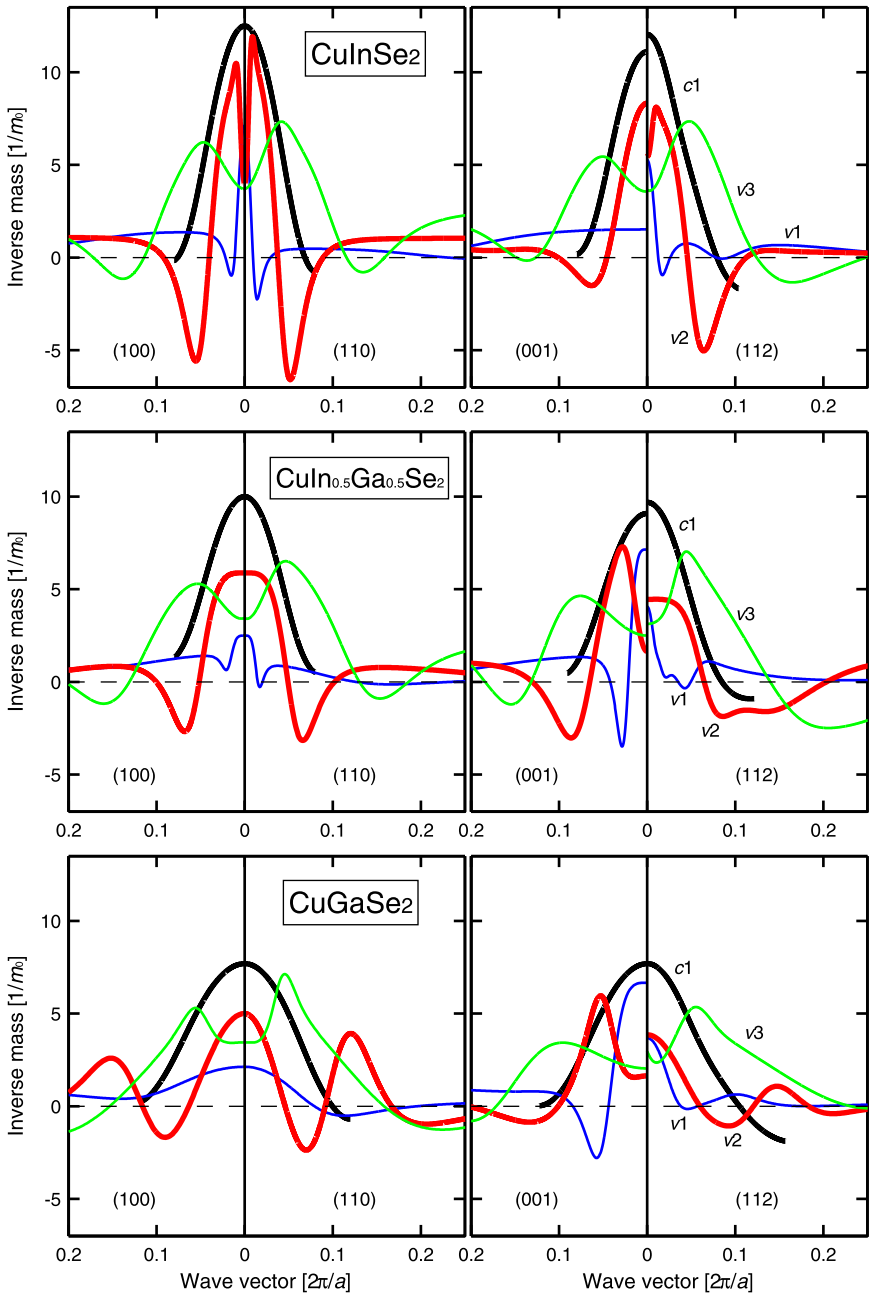

Fig. 3. Inverse of the effective electron and hole masses for $CuIn_{1-x}Ga_xSe_2$ ($x = 0$, 0.5, and 1) in the four symmetry directions as in Fig. 2, obtained from the second derivative of the energy dispersion: $m_j(\mathbf{k})^{-1} = \pm(\partial^2 E_j(\mathbf{k})/\partial\mathbf{k}^2)/\hbar^2$. The band indices ($j = c1, v1, v2$, and $v3$) refer to the energy bands in Figs. 1 and 2. The presented masses are the component parallel to the considered symmetry directions.

dispersion $E_j(\mathbf{k})$ is linear with respect to $\mathbf{k}$. Fig. 3 demonstrates a strong non-parabolicity of all the considered bands, that is, $m_j(\mathbf{k})^{-1}$ is not constant along each symmetry direction. Moreover, it is clear from the figure that the CB has a rather isotropic electron mass tensor at the Γ – point [thus, $m_{c1}^{100}(\mathbf{0}) \approx m_{c1}^{110}(\mathbf{0}) \approx m_{c1}^{001}(\mathbf{0}) \approx m_{c1}^{112}(\mathbf{0})$]; this is especially true for $CuGaSe_2$ whereas the electron mass of $CuInSe_2$ is somewhat anisotropic, as discussed also in Ref. [1]. The effective hole masses of the two topmost VBs ($j = v1$ and $v2$) show very strong anisotropy at the Γ-point [e.g., $m_{c1}^{100}(\mathbf{0}) \neq m_{c1}^{001}(\mathbf{0}) \neq m_{c1}^{112}(\mathbf{0})$]. However, for all bands and at the Γ-point, the inverse mass in the (110)-direction equals the inverse mass in the (100)-direction [thus, $m_j^{100}(\mathbf{0}) = m_j^{110}(\mathbf{0})$], conforming that we can use the notation transverse mass $m_j^{\perp} \equiv m_j^{100}$and longitudinal mass $m_j^{\parallel} \equiv m_j^{001}$ at the Γ-point.

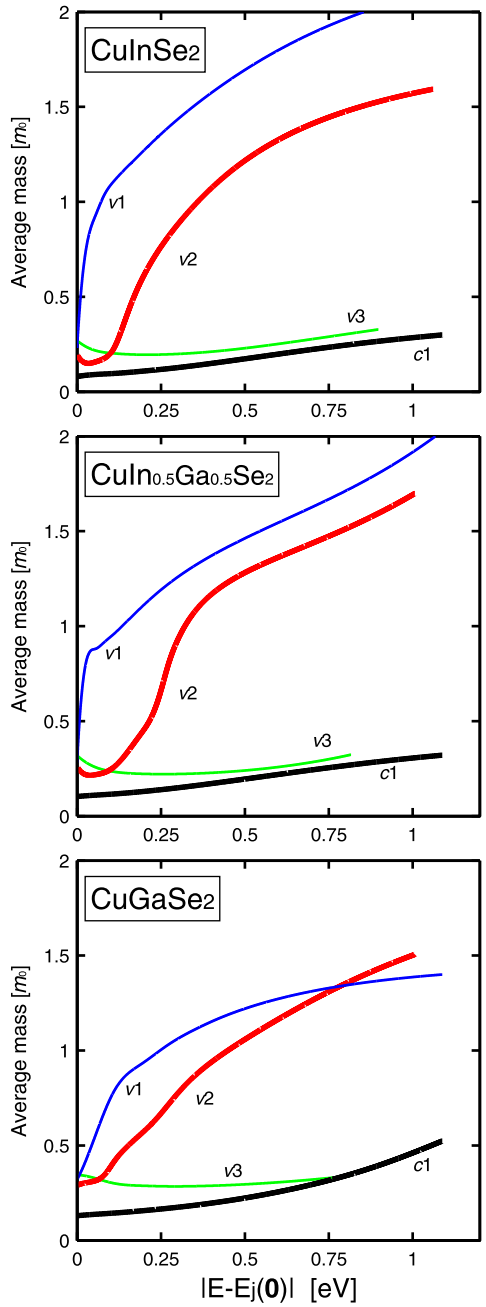

Fig. 4. The average energy-dependent masses of $CuIn_{1-x}Ga_xSe_2$ ($x = 0$, 0.5, and 1) to be used in analysis methods involving the parabolic approximation: $m_j(E) = \hbar^2(3\pi^2 N/V)^{2/3}/2|E - E_j(\mathbf{0})|$, where N is the number of energy states inside the constant energy surface for a crystal with volume V. The band indices ($j = c1$, $v1$, $v2$, and $v3$) refer to the energy bands in Figs. 1 and 2.

At the very Γ-point, the values of the electron masses $m_{c1}(\mathbf{k} = \mathbf{0})$ in Table 1 confirm our earlier theoretical results [1]. Moreover, for $CuInSe_2$ the calculated electron mass components $m_{c1}^{\perp} = 0.08\, m_0$ and $m_{c1}^{\parallel} = 0.09\, m_0$ verify the Faraday rotation data by Weinert et al. [9] $m_{c1} = 0.09\, m_0$ and Shubnikov-de Haas oscillation data by Arushanov et al. [10] $m_{c1} = 0.08\, m_0$. However, from Fig. 3, it is clear that the effective electron mass increases (i.e., inverse masse decreases) away from the Γ-point. This will affect the electron transport properties at high electric applied field. At $|\mathbf{k}| \approx 0.1 \cdot 2\pi/a$ the mass is infinity (i.e., $m_j(\mathbf{k})^{-1} = 0$). This occurs at about 0.3 eV above the CBM, reflecting that the CB starts to become more flat with a negative mass further out in the BZ (see Fig. 1). Our parameterized energy dispersion describes this effect on the mass, but it cannot describe the negative electron mass for $|\mathbf{k}| > 0.15 \cdot 2\pi/a$.

Since the spin-orbit coupling and the crystal field affect the VB curvatures near the Γ-point primarily, the uppermost VBs are strongly non-parabolic (Fig. 2), and this will directly affect the effective hole masses (Fig. 3). Hole masses of $CuGaSe_2$ vary somewhat less compared with those of $CuInSe_2$, mainly because $CuGaSe_2$ has larger split between the VBs. Overall, all the three $CuIn_{1-x}Ga_xSe_2$ compositions show comparable $\mathbf{k}$-dependency of their masses.

Due to the strong non-parabolicity, the Γ-point hole masses are strictly valid only close to the Γ-point, and can therefore not be used to describe band filling. We therefore present also an average energy-dependent effective mass $m_j(E)$ that can be employed in future analysis (Fig. 4). This mass can thus describe the quasi Fermi level $|E - E_j(\mathbf{0})|$ as function of band filling. From the figure, it is clear that one needs to consider the non-parabolicity of the two uppermost VBs when to analyze hole transport or band filling effects. For instance, $m_{v1}^{\perp} = 0.14\, m_0$ and $m_{v1}^{\parallel} = 0.66\, m_0$ in $CuInSe_2$ yield $m_{v1}(E \approx 0) = (m_{v1}^{\perp} m_{v1}^{\perp} m_{v1}^{\parallel})^{1/3} = 0.23\, m_0$. This mass increases drastically when E increases to about $1.00\, m_0$ at $E = 0.1$ eV. This can thus explain the large measured hole masses $m_{v1} \approx 0.7\, m_0$ in $CuInSe_2$ [11,12] since the indirect measurements involves high hole concentrations. Also analyses involving band filling of the CB need to consider the non-parabolicity since the m_{c1}(E) is increased by about a factor of 2 at energy $|E - E_{c1}(\mathbf{0})| = 0.5$ eV.

4. Summary

To summarize, the parameterization of the electronic band structure of $CuIn_{1-x}Ga_xSe_2$ ($x = 0$, 0.5, and 1) demonstrates that the energy dispersions of the lowest CB and uppermost VBs [that is, $E_j(\mathbf{k})$ with $j = v1$, $v2$, and $v3$] are strongly anisotropic and non-parabolic close to the Γ-point VBM $E_{v1}(\mathbf{0})$. This anisotropy and non-parabolicity directly affect the effective electron and hole masses.

Acknowledgements

This work is supported by the Swedish Energy Agency, the Swedish Research Council, the China Scholarship Council, and the computers centers NSC and HPC2N through SNIC/SNAC.

References

[1] C. Persson, Appl. Phys. Lett. 93 (2008) 072106.
[2] C. Persson, Thin Solid Films 517 (2009) 2374.
[3] E. Engel, S.H. Vosko, Phys. Rev. B 47 (1993) 13164.
[4] C. Persson, S. Mirbt, Br. J. Phys. 36 (2006) 286.
[5] O. Madelung (Ed.), Semiconductors - Basic Data, 2nd ed., Springer, Berlin, 1996.
[6] C. Persson, R. Ahuja, B. Johansson, Phys. Rev. B 64 (2001) 033201.
[7] J.M. Luttinger, W. Kohn, Phys. Rev. 97 (1955) 869.
[8] C. Persson, U. Lindefelt, J. Appl. Phys. 82 (1997) 5496.
[9] H. Weinert, H. Neumann, H.-J. Höbler, G. Kühn, N. van Nam, Phys. Status Solidi B 81 (1977) K59.
[10] E. Arushanov, L. Essaleh, J. Galibert, J. Leotin, M.A. Arsene, J.P. Peyrade, S. Askenazy, Appl. Phys. Lett. 61 (1992) 958.
[11] N.N. Syrbu, I.M. Tiginyanu, L.L. Nemerenco, V.V. Ursaki, V.E. Tezlevan, V.V. Zalamai, J. Phys. Chem. Solids 66 (2005) 1974.
[12] H. Neumann, W. Kissinger, H. Sobotta, V. Riede, G. Kühn, Phys. Status Solidi B 108 (1981) 483.